

Supporting information for

Synthesis of diethyl toluene diamine by zeolite-catalyzed ethylation of 2,4-toluene diamine

Yi Zuo¹, Xiaowa Nie¹, Min Liu¹, Ting Zhang¹, Chengyi Dai¹, Fanshu Ding¹, Chunshan Song^{2,},*

Xinwen Guo^{1,}*

¹ State Key Laboratory of Fine Chemicals, PSU-DUT Joint Center for Energy Research, Department of Catalysis Chemistry and Engineering, Dalian University of Technology, Dalian 116024, P. R. China.

² EMS Energy Institute, PSU-DUT Joint Center for Energy Research and Department of Energy & Mineral Engineering, Pennsylvania State University, University Park, PA 16802, USA.

Corresponding Authors

*C. Song. Tel.: +1 814 8634466; fax: +1 814 8653248; E-mail: csong@psu.edu

*X. Guo. Tel.: +86 411 84986133; fax: +86 411 84986134; E-mail: guoxw@dlut.edu.cn

The analysis of products by GC-MS, characterization of the zeolites, and DFT calculation of thermodynamic parameters, atomic charge and reaction barriers in vapor phase were settled in the supplementary information.

1 Gas chromatograph-mass spectrum analysis of the products

Gas chromatograph-mass spectrum (GC-MS) was obtained on a HP6890GC/5973MS system to analyse the products of 2,4-TDA ethylation. The GC profile of the reaction over nano-scaled HZSM-5 aggregate for 5 h is shown in Fig. S1. According to the MS data and the standard samples data obtained in GC, the peak at 17.5 min in Fig. S1 was assigned as 3,5-DE-2,4-TDA, while those at 16.8 and 15.5 min were 3,6-DE-2,4-TDA and 5,6-DE-2,4-TDA, respectively. The peak at 22.1 min was TETDA. The peaks between 5.8 and 6.2 min were the disproportionation products. The peak at 4.7 min was of 2,4-TDA, and that at 1.6 min was ethanol. Other peaks were N-ethylation products and so on. The mass spectrum of 3,5-DE-2,4-TDA is shown in Fig. S2.

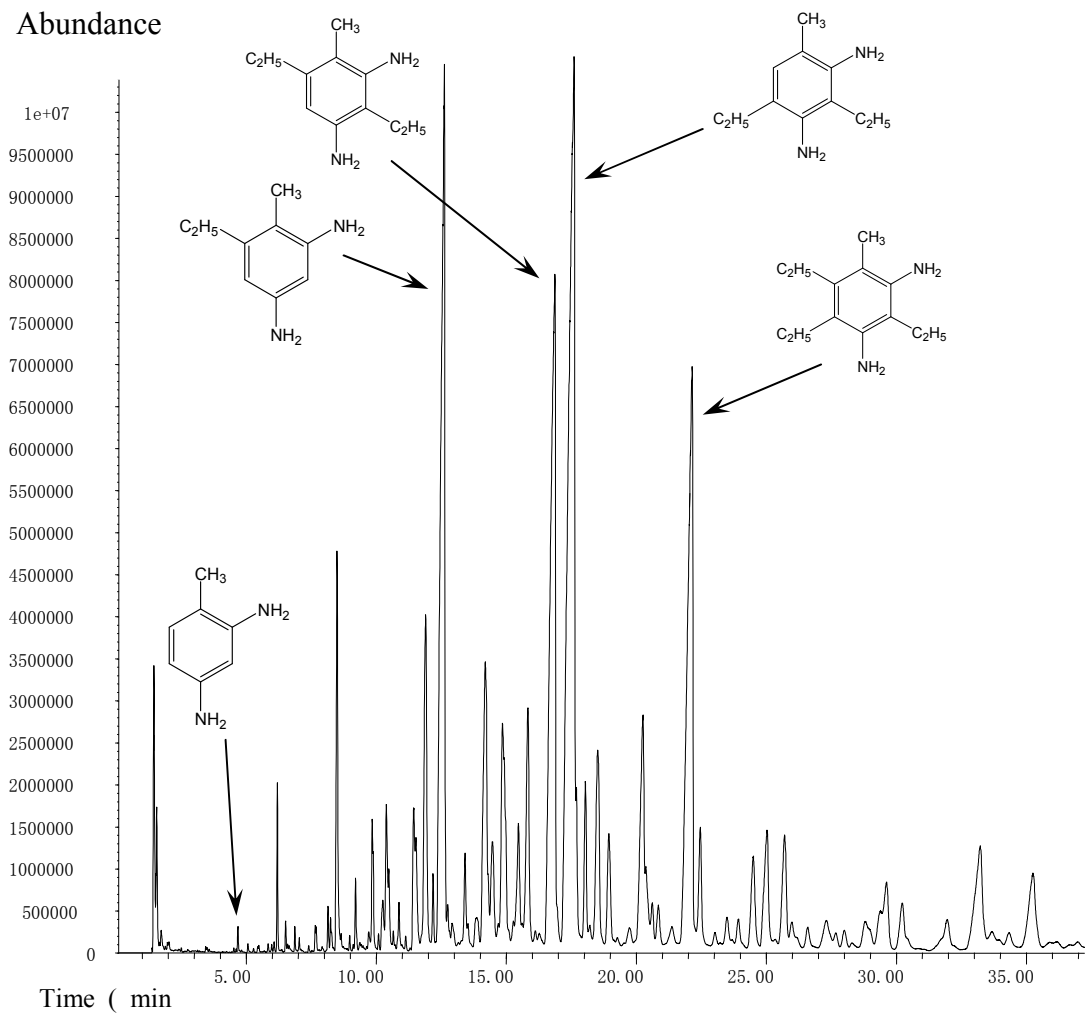


Figure S1. The GC-MS result of the products from ethylation of 2,4-toluenediamine over HZSM-5.

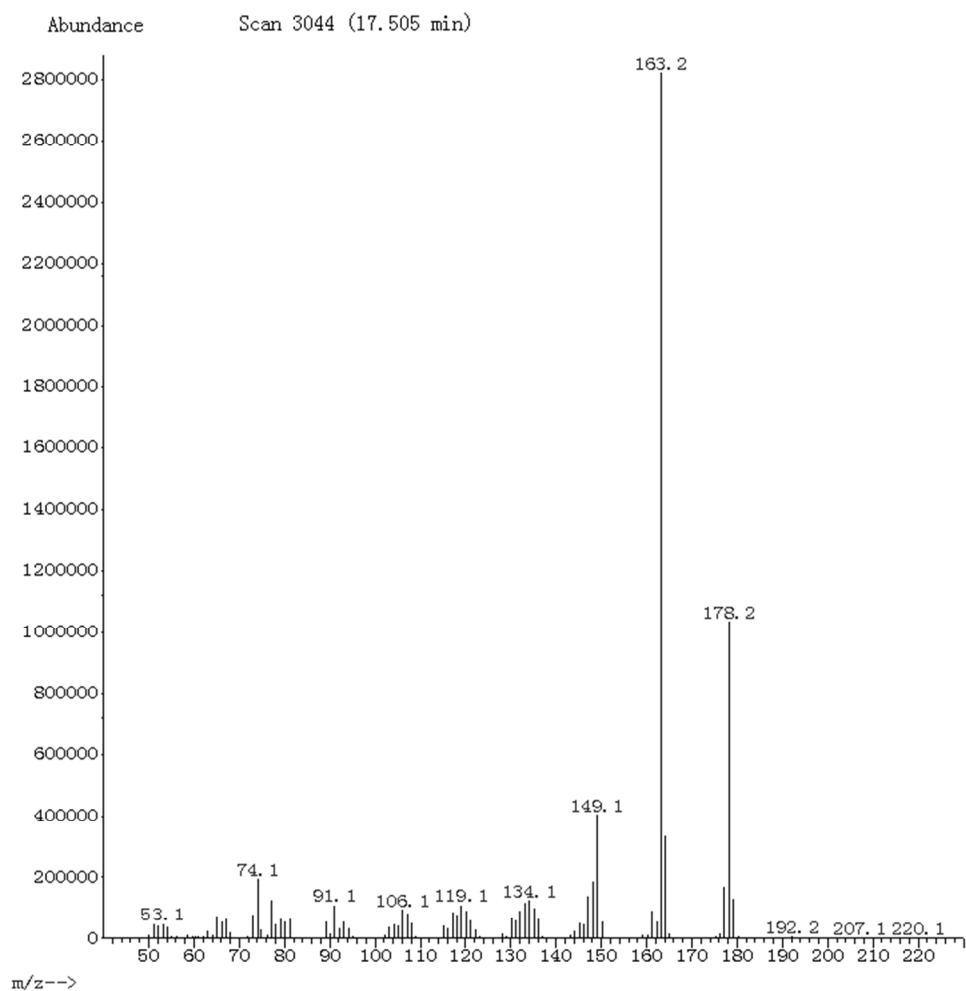


Figure S2. The mass spectrum of 3,5-diethyl-2,4-toluene diamine.

2 Characterization of zeolites

Figure S3 shows the XRD patterns of the zeolites, which were performed on a Rigaku Corporation SmartLab 9 X-ray diffractometer equipment using Cu K α radiation. Each pattern shows the typical characteristic peaks of the corresponding zeolite.

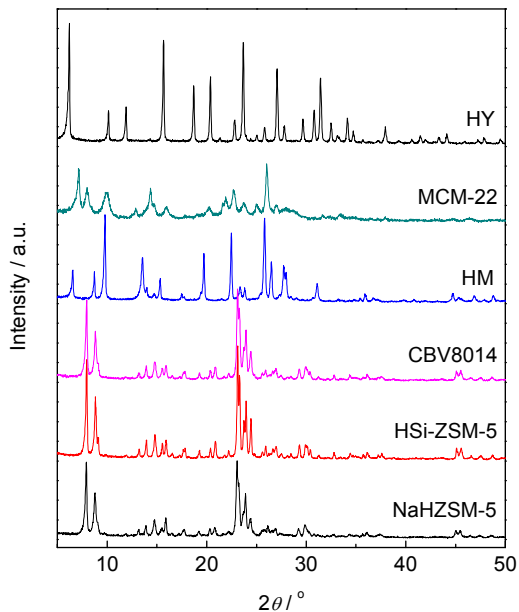


Figure S3. XRD patterns of the acidic zeolites.

Figure S4 shows the pore diameter distribution curves of the samples based on the argon physisorption. The test was carried out on a Quantachrome AUTOSORB iQ2 physical sorption apparatus at -186 °C.

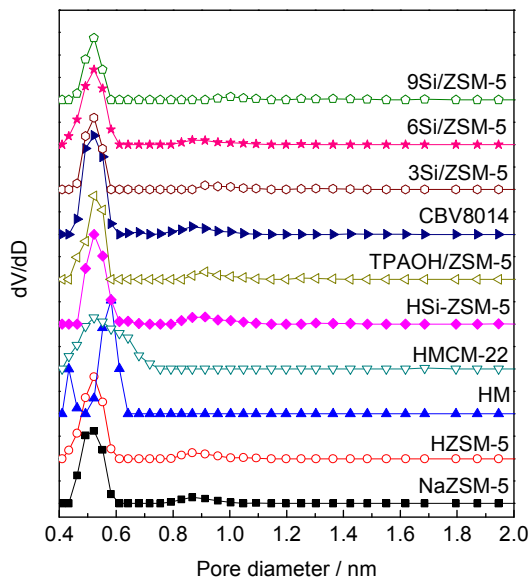
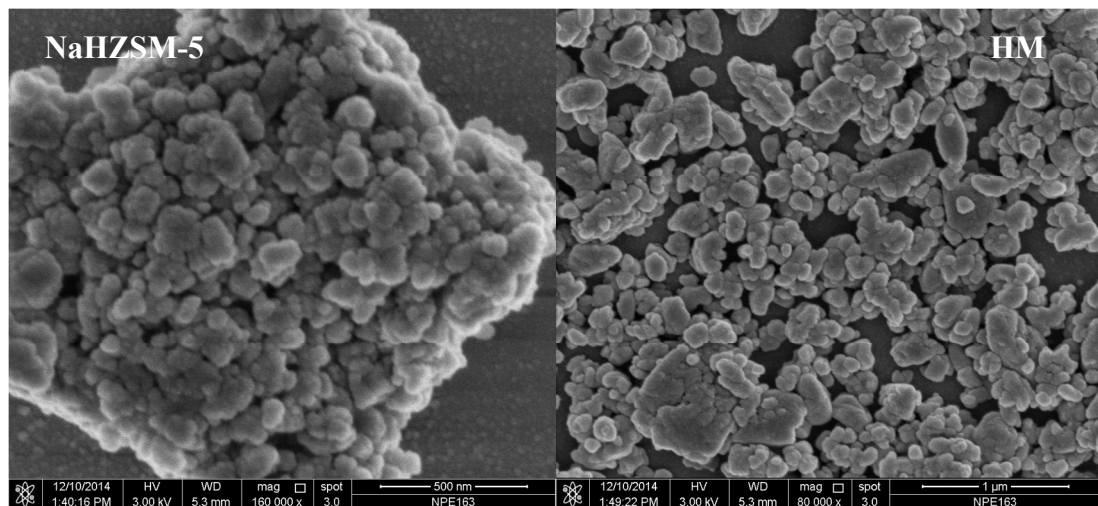


Figure S4. Pore diameter distribution of the acidic zeolites.

The appearances of some zeolites, which were determined on a Hitachi S-4800 scanning electron microscope, were shown in Fig. S5.



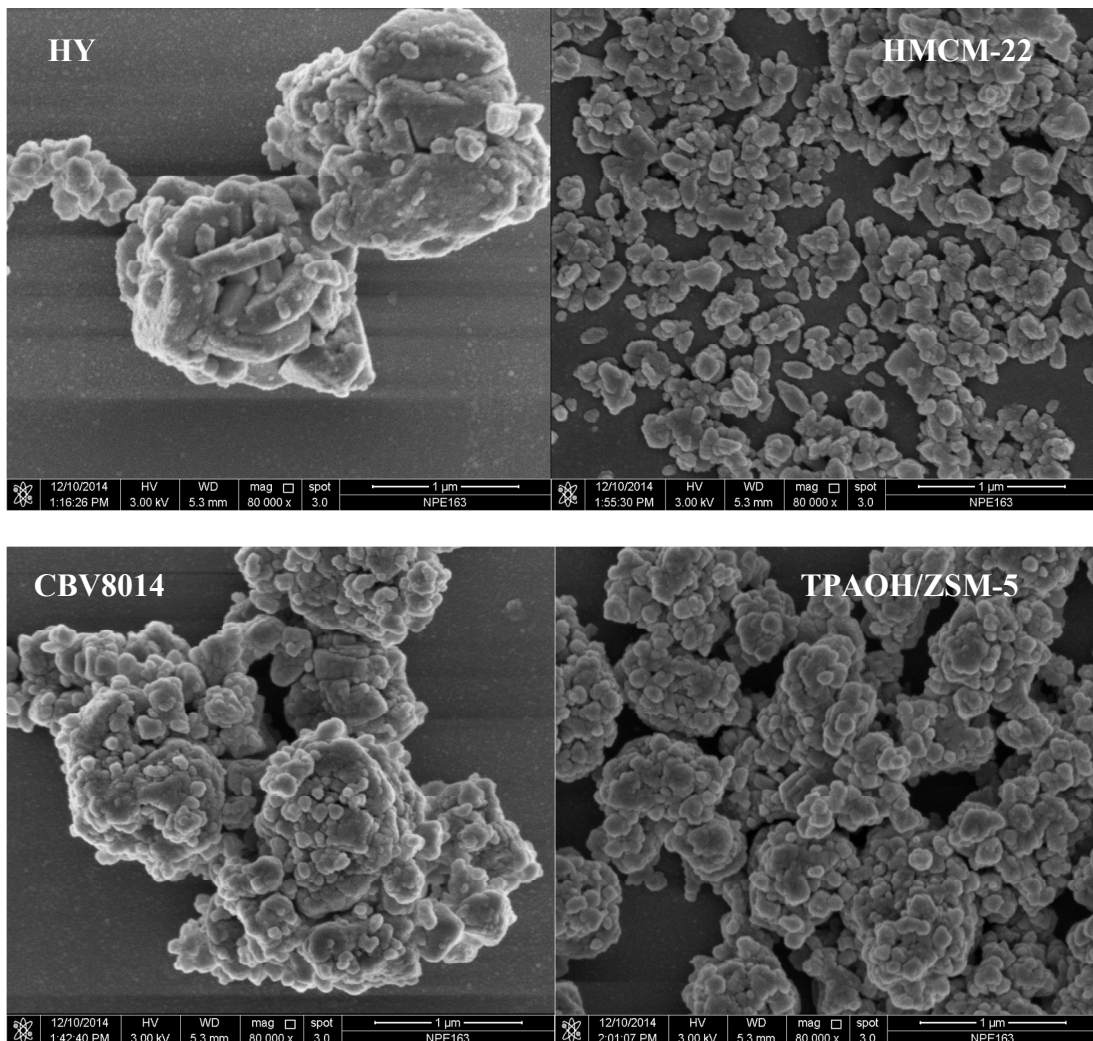


Figure S5. SEM images of some acidic zeolites.

3 Density functional theory calculation

The thermodynamic parameters, atomic charge and reaction barriers were calculated based on the optimized molecular geometries at a B3LYP/6-311++G(d,p) level of theory within the framework of DFT. All calculations were performed using the Gaussian 03 package.^{S1}

To understand the mechanism of the reaction as well as the optimal conditions that facilitate the DETDA manufacture, DFT calculation was applied. Fig. S6 gives partial atomic Mülliken

charge of 2,4-TDA. It shows that the electrophilic attack is prone to occur on nitrogen atom (N-ethylation) rather than on carbon atom (C-ethylation) in the benzene ring.

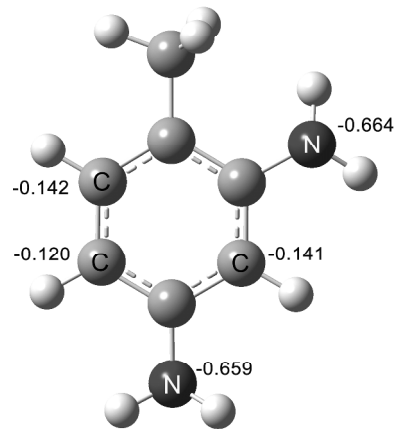


Figure S6. The structure and Mulliken charges of 2,4-toluene diamine.

The reaction enthalpy changing in contact with each possible product was evaluated and presented in Table S1. The C-ethylation is thermodynamically more favored than the N-ethylation, because the C-ethylation reactions are more exothermic. To gain fundamental insight into the kinetics for the ethylation reaction, we further calculated the activation barriers (E_a) for the mono-ethylation products, including the 3-, 5-C-products and 2-, 4-N-products in the gaseous phase (Fig. S7). Transition state configurations are shown in Fig. S8. E_a values indicate that the N-ethylation products formation is more preferred in kinetics with relatively lower barriers. The relative reaction rates of N-ethylation versus C-ethylation (denoted as k_N/k_C) at specific reaction temperature were evaluated in terms of the Arrhenius equation, and the results were 1154, 405 and 186 for 300, 400 and 500 °C, respectively. Presumably, the reaction temperature plays an

important role in this reaction. Increasing the temperature in a certain range would be helpful for C-ethylation.

Table S1. Thermodynamic parameters.

| Products | $\Delta H/\text{kcal}\cdot\text{mol}^{-1}$ | Electronic energy/Ha |
|------------------|--|----------------------|
| 3,5-C-ethylation | -43.5 | |
| 3-C-ethylation | -21.5 | -460.708584 |
| 5-C-ethylation | -22.4 | -460.710220 |
| 2-N-ethylation | -17.3 | -460.702111 |
| 4-N-ethylation | -18.5 | -460.703877 |

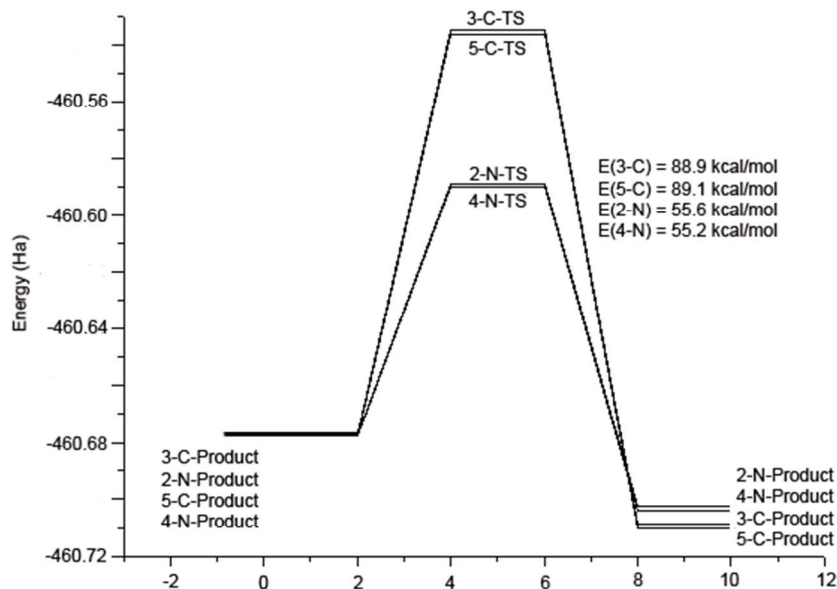


Figure S7. Schematic view of the electronic energies (E) for ethylation of 2,4-toluene diamine with ethene. The relative E values were obtained from B3LYP/6-311++G(d,p) calculations.

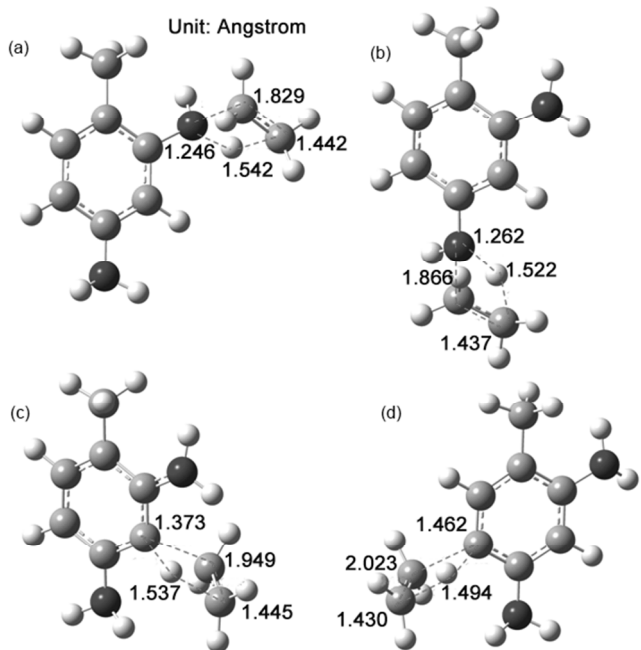


Figure S8. Transition state (TS) geometries for ethylation of 2,4-TDA: (a) 2-N-ethylation; (b) 4-N-ethylation; (c) 3-C-ethylation; (d) 5-C-ethylation.

In summary, the C-ethylation needs longer reaction time and higher temperature.

REFERENCES

(S1) M. J. Frisch, G. W. Trucks, H. B. Schlegel, G. E. Scuseria, M. A. Robb, J. R. Cheeseman, J. A. Jr. Montgomery, T. Vreven, K. N. Kudin, J. C. Burant, J. M. Millam, S. S. Iyengar, J. Tomasi, V. Barone, B. Mennucci, M. Cossi, G. Scalmani, N. Rega, G. A. Petersson, H. Nakatsuji, M. Hada, M. Ehara, K. Toyota, R. Fukuda, J. Hasegawa, M. Ishida, T. Nakajima, Y. Honda, O. Kitao, H. Nakai, M. Klene, X. Li, J. E. Knox, H. P. Hratchian, J. B. Cross, V. Bakken,

C. Adamo, J. Jaramillo, R. Gomperts, R. E. Stratmann, O. Yazyev, A. J. Austin, R. Cammi, C. Pomelli, J. W. Ochterski, P. Y. Ayala, K. Morokuma, G. A. Voth, P. Salvador, J. J. Dannenberg, V. G. Zakrzewski, S. Dapprich, A. D. Daniels, M. C. Strain, O. Farkas, D. K. Malick, A. D. Rabuck, K. Raghavachari, J. B. Foresman, J. V. Ortiz, Q. Cui, A. G. Baboul, S. Clifford, J. Cioslowski, B. B. Stefanov, G. Liu, A. Liashenko, P. Piskorz, I. Komaromi, R. L. Martin, D. J. Fox, T. Keith, M. A. Al-Laham, C. Y. Peng, A. Nanayakkara, M. Challacombe, P. M. W. Gill, B. Johnson, W. Chen, M. W. Wong, C. Gonzalez and J. A. Pople, *Gaussian 03 revision E.01*, Gaussian Inc., Pittsburgh, PA, 2003.